Remote Sensing Applications: Society and Environment 38 (2025) 101567

Contents lists available at ScienceDirect

Remote Sensing Applications: Society and Environment

journal homepage: www.elsevier.com/locate/rsase

Investigation of the Surface Urban Heat Island (SUHI) by two remote sensing-based approaches in Italian regional capitals

Gennaro Albini [a,*], Giulia Guerri [a], Michele Munafò [b], Marco Morabito [a]

[a] National Research Council, Institute of Bioeconomy (CNR-IBE), Via Madonna del Piano 10, 50144, Florence, Italy
[b] Institute for Environmental Protection and Research (ISPRA), 00144, Rome, Italy

ARTICLE INFO

Keywords:
Surface temperature
Surface Urban Heat Island
Land take
Remote sensing
Urban features

ABSTRACT

This study investigates the Surface Urban Heat Island (SUHI) phenomenon in the twenty Italian regional capitals for the 2013–2023 period by analyzing summer surface temperatures and urban features. Using open data from remote sensing products (such as Landsat-8 and 9 and Sentinel-1 and 2) as well as the Italian Revenue Agency database, this research examines surface temperature differences between central and peripheral urban areas. Two methodological approaches were employed: 1) the Real Estate Market Observatory classification provided by the Italian Revenue Agency (OMI approach) and 2) urbanization levels as defined by the Italian Institute for Environmental Protection and Research (urbanization level approach). High SUHI values were observed in cities with different geographical characteristics, including mountainous areas, with the highest values in L'Aquila, as well as both coastal and inland cities across plain and hilly altitudes. The highest SUHI intensities ranged from 5 °C to nearly 8 °C, with the urbanization level approach highlighting the most pronounced differences. Additionally, central urban areas in most regional capitals were characterized by over 60 % impervious surface coverage and minimal vegetation. Differences in tree cover percentages between urban belts showed significant positive relationships with SUHI intensity in both plain and hilly/mountainous cities. In particular, a highly significant ($p < 0.001$) positive linear relationship was found in plain cities: for every 10 % increase in tree cover differences between outer and central belts, SUHI intensity increased by about 1.0 °C. These findings provide valuable insights for public administrations planning urban development and reforestation aimed at mitigating extreme thermal conditions.

1. Introduction

The research produced by the international scientific community confirms the epoch-making scale of climate change and the increase in the intensity and frequency of extreme weather events (IPCC, 2022). These phenomena have evident impacts on biodiversity, ecosystems, and especially in urban areas due to the presence of multiple elements of vulnerability (Hjort et al., 2022; Seneviratne et al., 2021; Stolte et al., 2024). These include building and infrastructure characteristics, urban form, impervious surfaces, inadequate green infrastructure, and high population density. Recently, several regions in Europe have experienced a significant increase in the frequency and intensity of heatwaves (WHO, 2021), with the effects being particularly pronounced in the capitals of eastern and

* Corresponding author.
E-mail addresses: gennaro.albini@ibe.cnr.it (G. Albini), giulia.guerri@ibe.cnr.it (G. Guerri), michele.munafo@isprambiente.it (M. Munafò), marco.morabito@cnr.it (M. Morabito).

https://doi.org/10.1016/j.rsase.2025.101567
Received 13 December 2024; Received in revised form 11 April 2025; Accepted 18 April 2025
Available online 19 April 2025
2352-9385/© 2025 The Authors. Published by Elsevier B.V. This is an open access article under the CC BY license (http://creativecommons.org/licenses/by/4.0/).

Abbreviations

Abio =	Artificial abiotic surfaces
Tc =	Tree cover
Gc =	Grass cover
Nabio =	Natural abiotic surfaces
Wb =	Water bodies
LULC =	Land Use and Land Cover
ST =	Surface Temperature
SUHI =	Surface Urban Heat Island;
OMI =	Real Estate Market Observatory
PAs =	Public Administrations
a.s.l. =	above sea level
CNR- IBE =	National Research Council, Institute of Bioeconomy
ISPRA =	Institute for Environmental Protection and Research

southern EU countries (Morabito et al., 2018). Within urban areas, this thermal effect is further exacerbated by the anthropogenic phenomenon known as the Urban Heat Island (UHI), which induces a rise in local surface and air temperatures in densely populated cities compared to temperatures observed in rural regions (Akbari and Kolokotsa, 2016; Battaglia et al., 2017; Mirzaei et al., 2020). In this context, it is imperative to focus on urban settlement complexity regarding urban climate to mitigate the UHI and the Surface Urban Heat Island (SUHI).

Previous studies have employed various methodologies to estimate the SUHI phenomenon. For instance, data from MODIS Aqua, Sentinel-3, and Landsat 8 were used to compare day/night climatic conditions in Teheran and its suburbs to estimate the SUHI intensity (Zargari et al., 2024). In Granada (Spain) (Hidalgo-Garcìa and Arco-Dìaz, 2022), Landsat 5, 7 and 8 data were used to retrieve the surface temperature (ST) using the open-source software Qgis, estimating SUHI based on the temperature difference between urban and rural areas. Another study (Stewart et al., 2021) combined microscale and mesoscale urban climate models to analyze the diurnal SUHI cycle and spatiotemporal patterns, using satellite imagery datasets such as MODIS and Landsat. Moreover, a global long-term high-resolution dataset of daytime SUHI was developed using MODIS Aqua product and Sentinel-2, calculating SUHI as the temperature difference between built-up and surrounding rural areas (Mentaschi et al., 2022). The latest MODIS Collection-5 ST data was used to evaluate the geographic variations of the diurnal and seasonal SUHI phenomenon in China's 32 major cities (Zhou et al., 2014). In summary, remote sensing has advanced SUHI and UHI research by enabling spatiotemporal analysis while also addressing methodological challenges and knowledge gaps, as demonstrated by Phan et al. (2024). Despite these methodological advancements, accurately estimating SUHI still requires a strong focus on identifying urban centers within municipalities. In Italy, more than 70 % of the population lives in urban areas (The World Bank, 2024), where a significant increase in land take is amplifying the effects of the SUHI (Morabito et al., 2021). The net land take rate reached 19.4 ha per day in 2022, the highest recorded since 2012, marking a 10.2 % increase compared to 2021 and moving further away from the zero net land take targets (Munafò, 2023). This process is not slowing down but rather accelerating, often leading to the loss of natural and agricultural areas (Munafò, 2023).

As previously mentioned, several approaches exist for analyzing the SUHI phenomenon at the urban level. One method involves

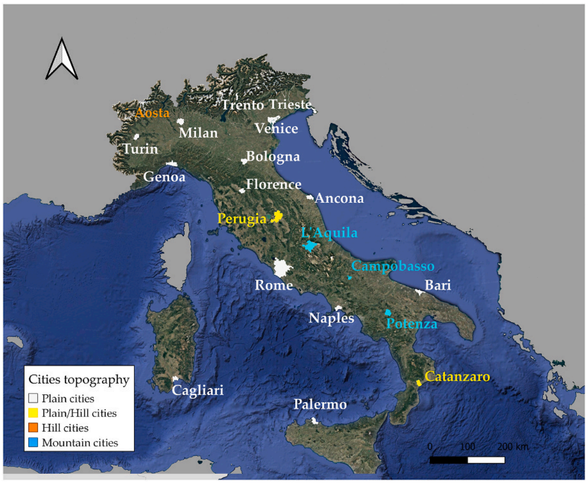

Fig. 1. Map showing the municipal areas of the twenty Italian regional capitals studied. City names and their administrative boundaries are color-coded according to the topography of their central areas.

assessing spatial and temporal variations in surface temperature (ST), which highlights temperature differences between the urban center and surrounding municipal areas, extending progressively towards the periphery (Dewan et al., 2021; Siswanto et al., 2023). This approach estimates SUHI intensity by measuring how much "warmer" the urban center is compared to peripheral areas. Another method involves evaluating SUHI based on land cover and urban land use (Yang et al., 2020; Zhao et al., 2017), emphasizing the role of impervious surfaces in urban surface thermal trends rather than classifying urban areas by their geographical distribution within the city.

Incorporating both methodologies, this study aims to analyze the presence and intensity of the summer SUHI phenomenon within the municipal territories of Italian regional capitals. Using high-resolution remote sensing data from Landsat-8 and 9 and Sentinel-2, the study examines variations in summer ST among different municipal areas, particularly between the urban center and outer areas. Additionally, it considers how varying urbanization density influences summer ST, accounting for various urban features such as impervious surfaces, tree cover, grasslands, and water bodies.

2. Materials and methods

2.1. Study-area

This study was carried out in Italy, focusing on the twenty Italian regional capitals (Fig. 1) over a period of about 10 years (2013–2023) during the summer season (June, July and August).

Italy spans the central Mediterranean, extending from approximately 36°N to 47°N latitude and covering an area of 301,340 km^2. This broad latitudinal range, combined with the influence of the surrounding Mediterranean Sea and the country's complex orography (dominated by the Alps and the Apennines) results in highly variable climatic and environmental conditions (Fratianni et al., 2017). Italy is particularly vulnerable to natural hazards, and climate change is expected to exacerbate this vulnerability in the coming decades (Fioravanti et al., 2022b; Giorgi and Lionello, 2008; Nicholls and Hoozemans, 1996). Current climate observations already confirm an increase in average temperatures, along with an increasing trend in extreme temperature events (Fioravanti et al., 2022a; Pisano et al., 2020). According to Köppen Climate Classification (Fratianni et al., 2017; Rubel and Kottek, 2010), the entire Italian peninsula falls within the Mediterranean climate zone, characterized by humid subtropical and temperate subtropical highland climates in the northern regions and hot-summer Mediterranean climates mainly in the central and southern regions.

2.2. Study framework and methodological approach

This study employed open-source data and software to investigate the SUHI phenomenon across the Italian regional capitals. Qgis (QGIS Development Team, 2023) and R environment (RStudio Team, 2020) were used for spatial and statistical analyses.

The study framework (Fig. 2) is organized into four main components.

2.2.1. Data sources

- Remote Sensing data from Landsat-8 and 9, and MODIS of the NASA missions, and Sentinel-1 and 2 of the Copernicus Programme.
- OpenStreetMap databases from the Real Estate Market Observatory (OMI) of the Italian Revenue Agency.
- Land Monitoring database from ISPRA.

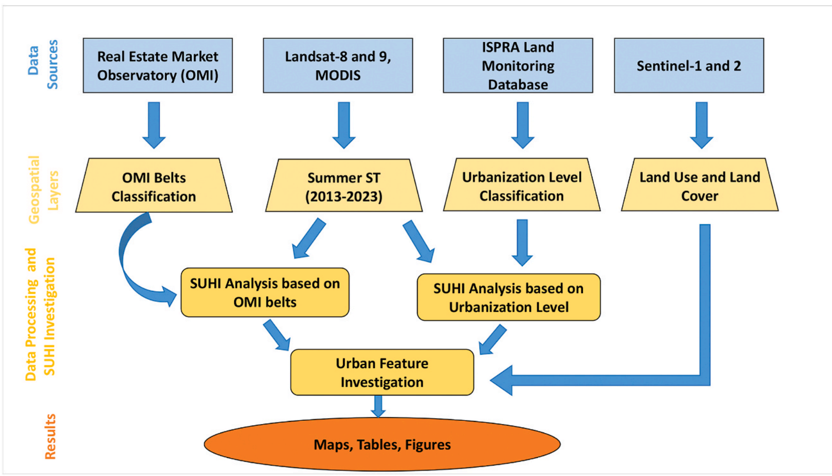

Fig. 2. Study framework and methodological approach.

2.2.2. Geospatial layers

- Daytime summer ST from Landsat-8 and 9, and MODIS imagery for the summer period from 2013 to 2023, with a spatial resolution of 60 m.
- OMI belts classification (central, semicentral, peripheral, suburban and extraurban).
- Urbanization level classification (urban, suburban, and rural).
- Land use and land cover (LULC) (tree cover, grasslands, impervious surfaces, water bodies) from ISPRA (De Fioravante et al., 2021), with a spatial resolution of 10 m.

2.2.3. Data processing and SUHI investigation

- SUHI analysis based on ST variations across different OMI belts, measuring ST differences between central and outer belts.
- SUHI analysis based on ST variations across different urbanization density levels, measuring ST differences between urban and other areas.
- Urban feature investigation across OMI belts and Urbanization level.

2.2.4. Results

- Figures, tables and maps that characterize and illustrate the SUHI phenomenon.

2.3. Surface temperature dataset

ST is a fundamental geophysical parameter for analyzing thermal behaviour and is widely used in SUHI studies (Grigoras and Uritescu, 2018; Guha et al., 2018; Guerri et al., 2021; Morabito et al., 2021).

In this study, the summer season was chosen due to the peak intensity of the SUHI phenomenon, primarily driven by daytime solar radiation, which results in significant temperature differences between urban centers and rural areas (Morabito et al., 2021; Esposito et al., 2024; Barbieri et al., 2018; Bonafoni et al., 2015). The survey period (2013–2023) was selected to ensure a robust dataset with consistent data acquisition across all cities.

Summer ST layers for the 2013–2023 period were selected from Landsat-8 and Landsat-9, and MODIS imagery, ensuring cloud cover remained below 60 %. Satellite images for summer ST analysis were processed using the Google Earth Engine platform (GEE). Specifically, ST was derived from the thermal infrared band 10 (TIRS) of the Collection 2 Level 1 Sensor, incorporating:

- Top Of Atmosphere (TOA) reflectance data and brightness temperature data;
- Advanced Spaceborne Thermal Emission and Reflection Radiometer (ASTER) Global Emissivity Dataset (GED) and Normalized Difference Vegetation Index (NDVI) data;
- Atmospheric reanalysis data, including geopotential height, specific humidity, and air temperature.

For each band within the municipalities under scrutiny, the average ST was computed. ST values for water bodies were excluded to evaluate the SUHI phenomenon focusing on ground ST. The main water bodies were identified by using seasonal land cover mapping provided by ISPRA and referring to summer surface water bodies, following the methodology described in De Fioravante et al. (2021) and made by Sentinel-2 data from the Copernicus Programme.

2.4. Real Estate Market Observatory (OMI) approach

This study utilized the classification system of the Italian Real Estate Market of the Italian Revenue Agency, that is the Real Estate Observatory (in Italian: Osservatorio del Mercato Immobiliare, OMI).

The OMI categorizes areas primarily into urban zones, which are contiguous sections of the municipal territory exhibiting homogeneity in positional, urban, historical-environmental, and socio-economic characteristics. These include factors such as the presence and accessibility of facilities and services, urban and suburban transport services, morphological-environmental conditions, and local population density (Festa et al., 2017).

Furthermore, homogeneous and contiguous zones can be aggregated into "belts", representing OMI zones with a specific geographical location. The entire municipal territory can thus be divided into *Central, Semicentral, Peripheral, Suburban* and *Extraurban* belts. The central belt corresponds to the municipal area comprising the urban center, characterized by a distinguishable perimeter of built structures exerting attraction toward larger settlements. The semicentral belt lies between the central and peripheral belts, directly connected to the urban center by services, transport, and infrastructure. The peripheral belt is bordered by the semi-central belt and is limited by the outer margin of the main urban agglomeration by undeveloped areas or natural/artificial barriers.

Each city's municipal area was mapped using vector data freely available from the Italian Revenue Agency. Summer ST differences between urban and peripheral areas were analyzed, providing a quantification of the SUHI phenomenon.

Data collection and geospatial analysis were conducted using the Qgis software. Additionally, topographical classification was performed using a 20 m Digital Elevation Model (DEM) from ISPRA, categorizing cities into plains (<300 m a.s.l.), hills (300–600 m a.s.l.), and mountains (>600 m a.s.l.), according to the Italian National Institute for Statistics (ISTAT - Italian National Institute of

Statistics, 2024).

Among the twenty cities investigated, fourteen are situated in plains, three are in hilly areas and three are in mountainous regions (Fig. 1). Additionally, nine cities are classified as coastal cities because their central or outer belts lie within 2 km of the coastline; these include: Ancona, Bari, Cagliari, Catanzaro, Genoa, Naples, Palermo, Trieste, and Venice. The remaining eleven cities are considered inland cities; these include: Aosta, L'Aquila, Bologna, Campobasso, Florence, Milan, Perugia, Potenza, Turin, Trento, and Rome (the latter considered a hybrid city since its municipality extends from the sea to over 20 km inland).

For cities like Catanzaro and Perugia, which include both plains and hilly areas in their urban centers (i.e. central belts), altitude-specific analyses were conducted. In all other cases where the OMI methodology was applied, the altitude of the central belt was adopted as the primary reference, with the altitudes of adjacent and peripheral areas subsequently considered.

2.5. Urbanization level approach

This study also employed a geospatial approach by analyzing the territories of municipalities based on their urbanization level. This method relied on 2021 raster data of artificialization levels, derived from land cover classifications, and provided by ISPRA at 10 m spatial resolution.

ISPRA's methodology for representing urban areas is based on delineating different types of urban fabric by considering only the spatial distribution of land use and land cover, with a focus on the average density of artificial surfaces. Urbanization levels were determined by reclassifying focal statistics derived from historical land take datasets. Specifically, three artificial surface density thresholds were established to distinguish between (Munafò, 2023):

- Urban areas (>50 %).
- Suburban areas (10–50 %).
- Rural areas (<10 %).

Each municipal area within the regional capitals was spatially classified into urban, suburban and rural zones, using raster data available for download from the National Environmental Information System (SINA) website. This classification was performed using

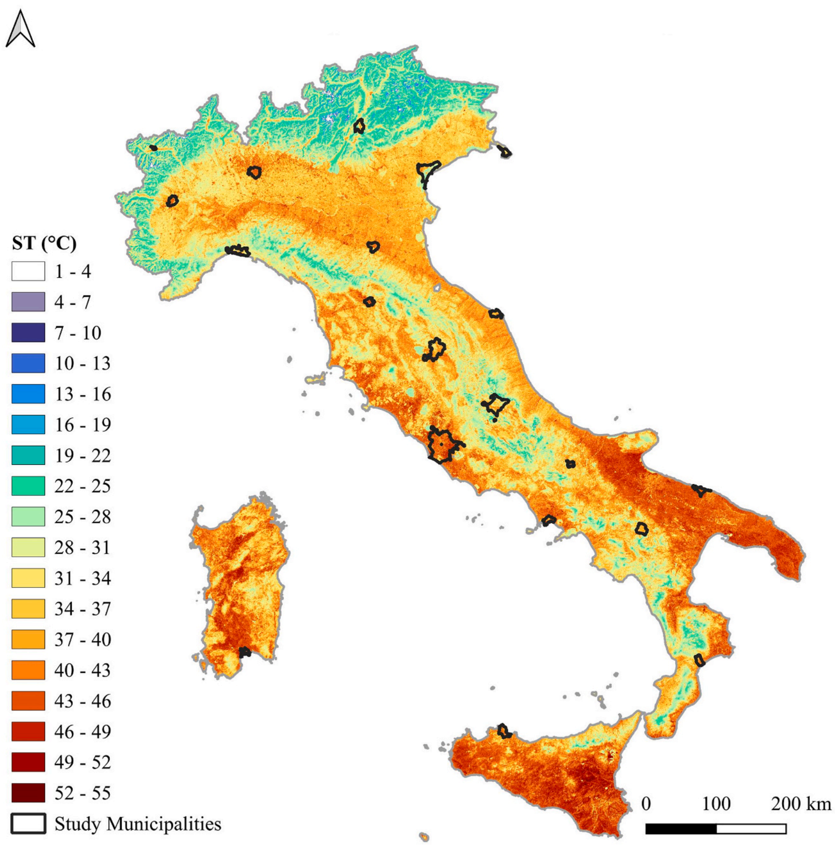

Fig. 3. The average summer Surface Temperature (ST) for the period 2013–2023 across the national territory of Italy. The study areas, corresponding to the regional capitals, were highlighted in black on the map.

the open-source software Qgis. The SUHI phenomenon was analyzed by extracting summer ST values for each urbanization level to assess thermal pattern differences between urban and suburban, and rural areas. This approach compares average ST values between highly anthropized areas, where land consumption density is very high, and other areas, without classifying them based on their specific spatial distribution within the urban context. This methodology enables a detailed investigation of the role that impervious surfaces play in driving thermal variations across different city zones (Saha et al., 2021).

2.6. Land use and land cover classification

The Italian regional capitals were further analyzed by characterizing both OMI belts and urbanization levels using land cover and use data. The land cover layer used in this study is based on ISPRA's national-scale land cover dataset. This classification system was obtained through the classification of Copernicus Sentinel-1 and Sentinel-2 satellite data, applying a specific methodology recently developed by De Fioravante et al. (2021, 2022).

The study used the following land cover layers at a 10-m spatial resolution:

- Artificial abiotic surfaces (hereafter named Abio);
- Natural abiotic surfaces (Nabio);
- Tree cover (Tc);
- Grass cover (Gc);
- Water bodies (Wb).

Urban characterization within each municipality was performed by using R and QGIS software.

3. Results

3.1. ST products

The national average summer ST values for the study-period 2013–2023 are shown in Fig. 3.

In areas where Landsat data were unavailable, MODIS data were used. *However, for the study areas considered (i.e., the regional capital municipalities), the Landsat data provided almost complete coverage, with MODIS data accounting for less than 1 % of the total area. This gap affected only one municipality (L'Aquila). The final spatial resolution (60 m) represented a reliable balance between the 30 m resolution of Landsat-8 and Landsat-9 data (provided by NASA) and the* 1 km *resolution of MODIS data.*

3.1.1. ST analysis of OMI urban belts

Fig. 4 displays the SUHI intensity across all twenty Italian regional capitals, as derived using the OMI belt approach. For Catanzaro and Perugia, only the SUHI intensity of the plan area is shown, given that these areas constitute over 50 % of the respective municipal territories and are therefore the most representative spatial units.

Among the cities with the highest mean ST values in the central belt were Florence (44.1 °C), Bologna (44.0 °C), and Aosta (43.7 °C) (Supplementary Materials, Table S1). In contrast, the cities with the lowest values in the central belt were Ancona (37.5 °C) and the plain of Catanzaro (37.5°) (Supplementary Materials, Table S1).

The SUHI intensity, defined as the ST difference between the central belt and the outer belts (semicentral, peripheral, suburban and extraurban), was found to be positive in most Italian regional capitals, except for Bari, the plain area of Catanzaro, Cagliari, and Rome (Figs. 4 and 5).

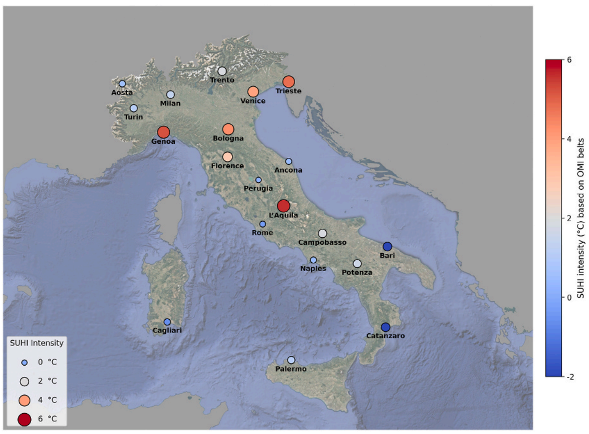

Fig. 4. SUHI intensity (°C) based on the OMI belt approach across Italian regional capitals.

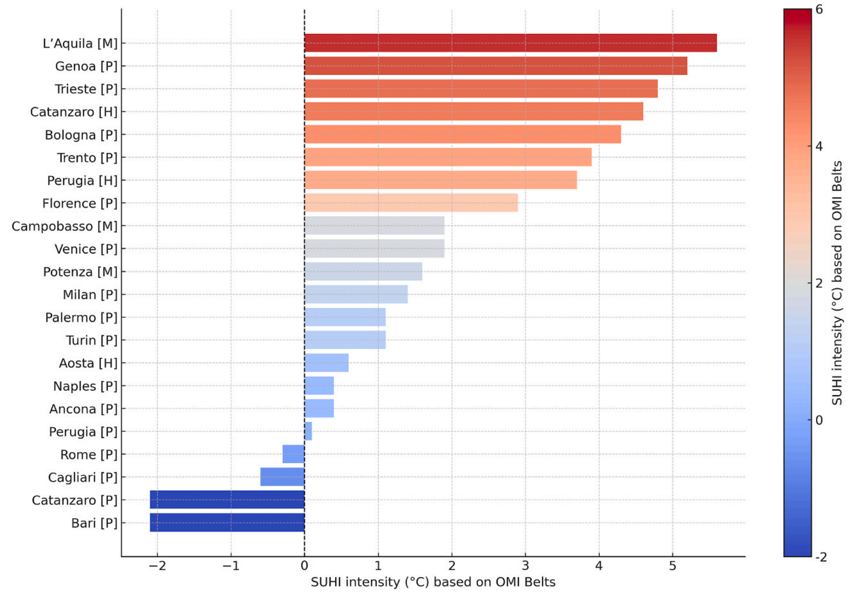

Fig. 5. The SUHI intensity calculated for the Italian cities studied through the "OMI belt" approach. Altitudinal indications are also provided in square brackets: [P] for plain, [H] for hilly, [M] for mountainous.

Among coastal cities, the SUHI phenomenon was particularly intense (SUHI intensity above 2 °C) in the plain areas of Genoa (5.2 °C) and Trieste (4.8 °C) (Figs. 4 and 5), as well as in the hilly area of Catanzaro (4.6 °C) (Fig. 5). Conversely, an inverse pattern was observed in the plain areas of Cagliari (−0.6 °C) and, notably, in Catanzaro (−2.1 °C) and Bari (−2.1 °C), where the central belt exhibited lower ST values than the outer belts (Figs. 4 and 5). In Bari, the suburban and extraurban belts revealed the highest ST values (43.0 °C and 44.9 °C) surpassing all other municipalities (Supplementary materials, Table S1).

Among inland cities, SUHI intensity was particularly high (above 2 °C) in L'Aquila (5.6 °C), Bologna (4.3 °C), Trento (3.9 °C), the hilly area of Perugia (3.7 °C), and Florence (2.9 °C).

Furthermore, when the cities were grouped into center-north and southern categories, SUHI intensity was more pronounced in center-north cities (above 2 °C) than in those located in the south (Fig. 5 and Supplementary Materials, Table S1).

When considering only the outermost belts (suburban and extraurban), the highest mean summer ST differences relative to the central belts were observed in Genoa (8.7 °C), Turin (8.1 °C), and Trieste (8.1 °C) (Supplementary Materials, Table S1). Similarly, pronounced differences were also noted in Milan (4.3 °C), Bologna (3.9 °C), Trento (3.7 °C), Palermo (2.2 °C), and Venice (1.9 °C) (Supplementary Materials, Table S1).

3.1.2. ST analysis by urbanization level

Fig. 6 displays the SUHI intensity across all twenty Italian regional capitals, as derived using the urbanization level approach. Also in this case, for Catanzaro and Perugia, only the SUHI intensity of the plain area is shown.

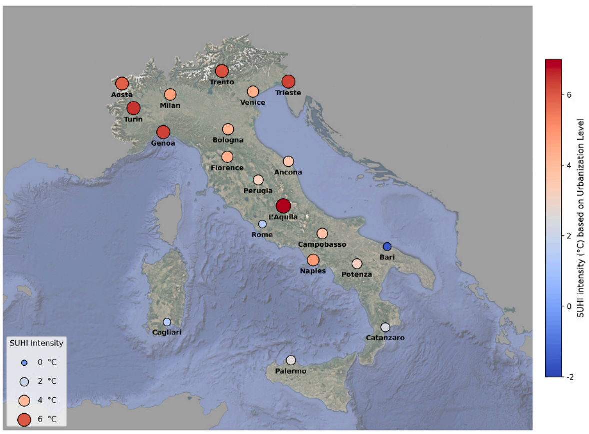

Fig. 6. SUHI intensity (°C) based on the Urbanization level approach across Italian regional capitals.

In general, regional capitals exhibited higher average ST in urban areas compared to their surrounding suburban and rural areas (Supplementary Materials, Table S2). The highest mean ST values were observed in Florence (44.0 °C), followed by Rome and Aosta (43.6 °C), while the lowest values were observed in Potenza and Trieste (39.4 °C), as well as in the hilly areas of Catanzaro (39.3 °C) and Perugia (39.4 °C) (Supplementary Materials, Table S2).

Regarding SUHI intensity, most cities revealed values around or above 3 °C (Figs. 6 and 7). However, Bari, exhibited an inverse trend (Figs. 6 and 7), with its urban area showing lower mean ST (−1.6 °C) compared to its suburban and rural areas.

The SUHI phenomenon was particularly intense (SUHI intensity above 5 °C) in L'Aquila (7.8 °C), Turin (6.5 °C), Genoa (6.3 °C), Trieste (6.3 °C), Trento (6.1 °C), Aosta (5.9 °C), and the hilly area of Catanzaro (5.1 °C) (Fig. 7). SUHI intensity was generally more pronounced in inland cities than in coastal ones (Fig. 7 and Supplementary Materials, Table S2).

Additionally, greater differences emerged when comparing ST values between urban and rural ones, regardless of geographical location (Supplementary Materials, Table S2). When cities were stratified by geographical location (north, center, and south), the center-north group exhibited the highest ST differences between urban and rural areas. Notably, Aosta (13.5 °C), Turin (8.4 °C), Trento (8.2 °C), Trieste (8.2 °C), Genoa (8.1 °C), Milan (6.9 °C), Florence (6.2 °C), and Bologna (5.9 °C) displayed the most important differences (Supplementary Materials, Table S2).

Between the two approaches, the classification based on the urbanization level showed the highest ST differences and SUHI intensity for the cities analyzed.

3.2. Urban feature investigation

Figs. 8 and 9 display the land cover percentages for each municipality, according to both the OMI and the Urbanization level approaches. The analysis focused primarily on Abio, Tc, and Gc, as these are key factors influencing the SUHI phenomenon. The central areas and, where available, the outermost ones, were considered.

The central belts exhibited a very high percentage of Abio (Fig. 8), nearly covering the entire land surface. This was particularly evident in Bologna (98.5 %), Genoa (94.5 %), Turin (94.3 %), Palermo (93.6 %) and Trieste (90 %). Almost all these cities also showed the highest SUHI intensity. The lowest Abio percentages were in Ancona, Catanzaro and Perugia (Fig. 8), although they still exceeded 50 % of total land coverage. For most of the cities, the percentage of Abio significantly decreased from the central belts to the outermost belts (suburban and extraurban), while the percentages of green coverage (Gc and Tc) increased. This trend was particularly evident in Genoa and Trieste (Fig. 8) where Tc increased from approximately 2 % in the central belt to 80 % in the suburban and extraurban belts. These cities also exhibited intense SUHI effects.

Similar patterns were observed in both coastal and inland cities (Fig. 9) when comparing the percentages of Abio, Tc, and Gc in urban areas versus suburban and rural areas.

Fig. 10 shows the relationship between SUHI intensity (°C) and Tc percentage differences between central and outer belts for cities located in plains with a positive SUHI intensity, based on the OMI belt approach.

Despite variations in size, morphology, and other urban characteristics, these cities were specifically selected to evaluate the relationship between SUHI intensity and tree cover, considering topographical factors.

The linear regression for plain cities in Fig. 10 showed that approximately 70 % of the variation in SUHI intensity can be explained

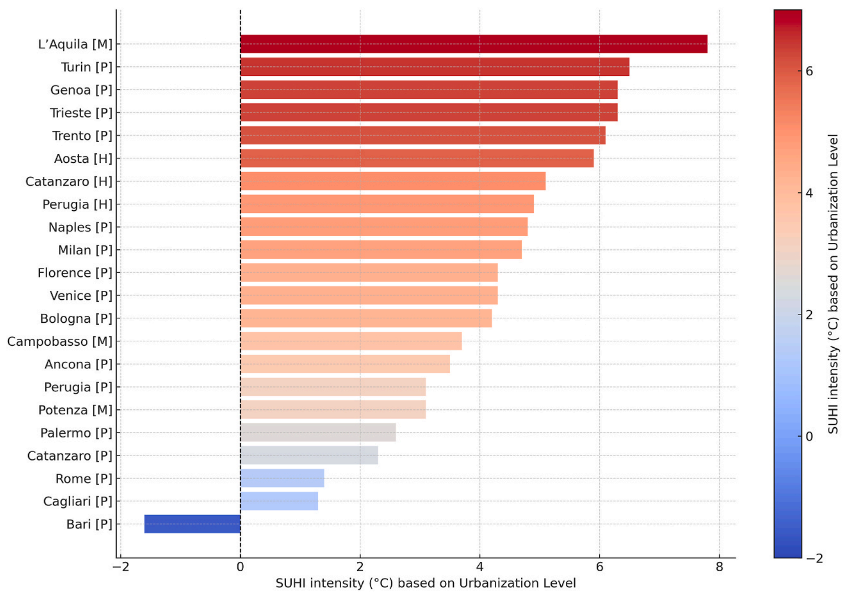

Fig. 7. The SUHI intensity calculated for the Italian cities studied by the "Urbanization Level" approach. Altitudinal indications are also provided in square brackets: [P] for plain, [H] for hilly, [M] for mountainous.

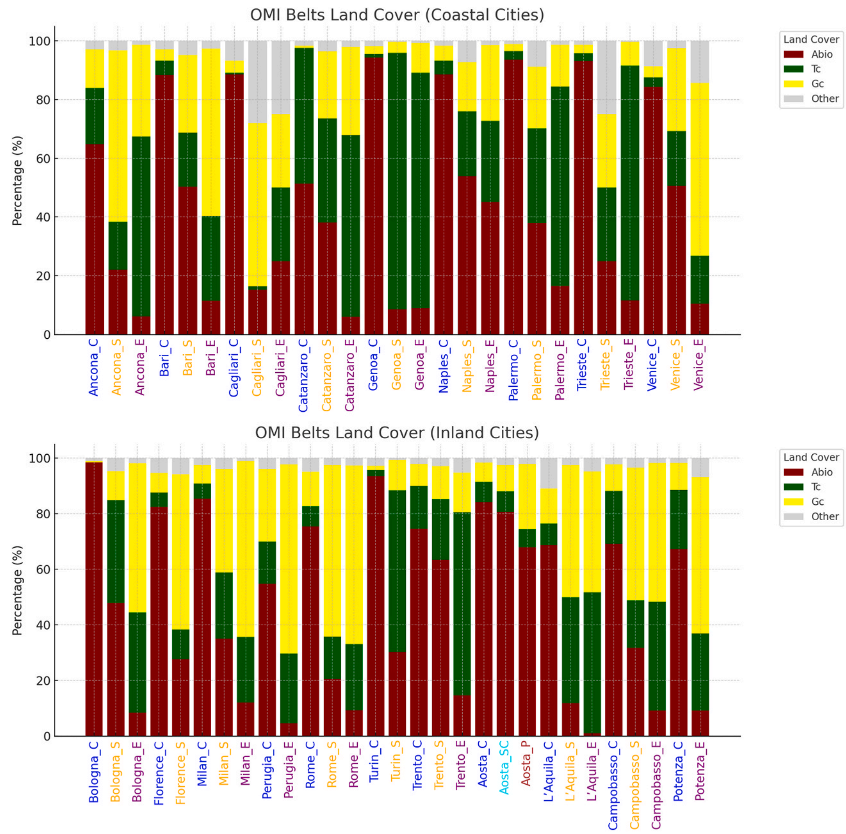

Fig. 8. Description of the percentages of artificial abiotic surfaces (Abio, red), tree cover (Tc, green), grass cover (Gc, yellow), and water bodies plus natural abiotic surfaces (Other, grey) for the central (C) and outer (S, suburban; E, extraurban) OMI belts of coastal and inland municipal capitals.

by differences in *Tc* percentages between outer and central belts ($R^2 = 0.70$). This indicates a highly significant ($p < 0.001$) positive linear correlation: for every 10 % increase in Tc differences between outer and central belts, SUHI intensity rises by about 1.0 °C.

Fig. 11 shows the same relationship for hilly and mountainous cities, where a significant positive correlation was also observed ($p < 0.05$), confirming the influence of tree cover on SUHI intensity in these areas according to the OMI approach.

Additional analyses assessed the relationship between SUHI intensity and Tc differences for both plain and hilly/mountainous cities, using the urbanization level approach. These relationships showed lower significance ($p < 0.05$) for plain cities, and a negligible linear relationship for hilly and mountainous cities (Supplementary Materials, Figs. 1 and 2), compared to the OMI approach.

4. Discussion

Both methodologies employed proved valuable in investigating the SUHI phenomenon at the regional capital level. Their application enabled the estimation of the SUHI phenomenon both in the classical sense, by determining how much warmer the urban center is compared to the surrounding areas (Oke, 1987), and by assessing the thermal impact of urbanization within the studied cities. Specifically, it was observed that areas with higher land consumption density exhibited higher temperatures than less urbanized areas, regardless of their location within the municipality.

The OMI methodology highlighted that the SUHI phenomenon is evident in almost all regional capitals.

Although varying in intensity, the most pronounced SUHI values were found in the central and northern municipalities, such as L'Aquila, Genoa, Trieste, and Turin. The results also revealed that for some southern coastal municipalities, and in particular for Bari (confirmed by both approaches to investigate SUHI), the SUHI phenomenon was reversed.

This finding aligns with a recent study (De Razza et al., 2024) that observed a similar reverse effect in Salento, Puglia, near the Bari municipality. Our study suggests that the low percentage of tree cover in outer areas (generally not exceeding 20 %), much lower than the 40 % or more observed in cities exhibiting high SUHI effects, contributes to this reverse effect. Additionally, the reflective properties of building material, such as a local limestone found in historical sectors of Salento's cities, likely play a role, as reported by De Razza et al. (2024). The positive linear relationships observed in our analysis suggest that larger differences in tree cover between outer and central areas are linked to higher SUHI intensity.

Moreover, given that all these cities are coastal, this phenomenon could be explained by the proximity of central belt to the sea (Firozjaei et al., 2023; Morabito et al., 2021). Additionally, nearshore areas may be affected by surface moisture, which is considered a

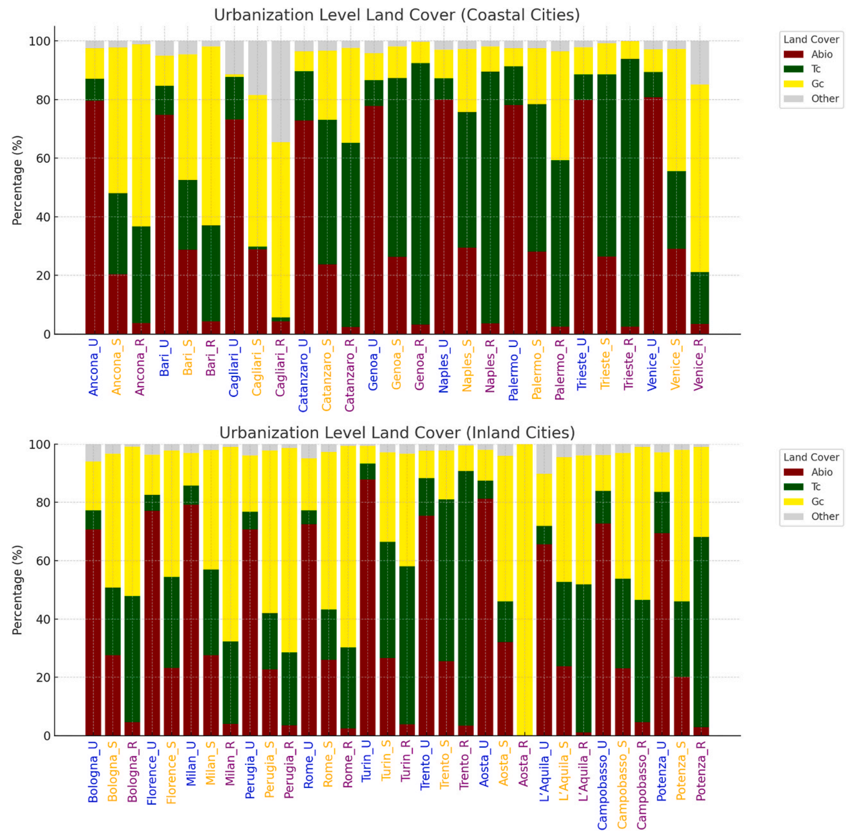

Fig. 9. Description of the percentages of artificial abiotic surfaces (Abio, red), tree cover (Tc, green), grass cover (Gc, yellow), and water bodies plus natural abiotic surfaces (Other, grey) for urban (U), suburban (S) and rural (R) areas calculated through the Urbanization level approach of coastal and inland municipal capitals.

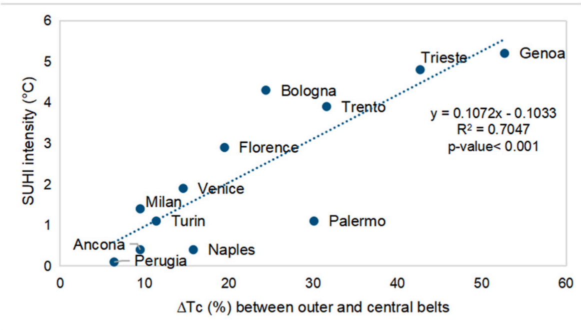

Fig. 10. Relationships between the Surface Urban Heat Island (SUHI) intensity calculated through the OMI belt approach and tree cover (Tc) percentage differences (between outer and central belts) for plain cities. Statistical significance (p-value <0.001) refers to the linear relationship.

potential factor influencing ST variation (Roberts et al., 2012). The cooling effect of proximity to the sea varies across cities and their morphological characteristics, but previous studies have also demonstrated a relationship between increasing ST and distance from the coastline(Guo et al., 2023). This is especially true for Bari, where suburban and extraurban belts are approximately 11 km from the coast.

These considerations change for most of the aforementioned cities when using the urbanization level to assess intra-urban ST differences. In this case, almost all the urban areas were found to have higher ST than other areas, confirming that high land consumption density impacts the SUHI phenomenon.

The characterization of land cover using both the OMI and the urbanization level approaches has also been valuable for quantifying the percentage of impervious surfaces (Abio) and green cover (Tc and Gc), both of which play key roles in the SUHI phenomenon.

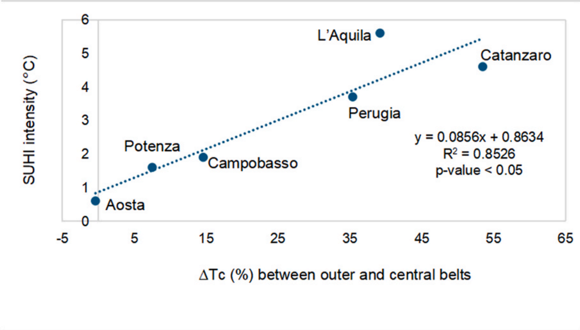

Fig. 11. Relationships between the Surface Urban Heat Island (SUHI) intensity calculated through the OMI belt approach and tree cover (Tc) percentage differences (between outer and central belts) for hilly and mountainous cities. Statistical significance (p-value <0.05) refers to the linear relationship.

Particularly, Tc contributes significantly to improving the urban microclimate and mitigating SUHI (Adeyeri et al., 2017; Marando et al., 2022; Ribeiro et al., 2023; Tan et al., 2016). Our findings indicate that Tc is strongly associated with SUHI intensity in cities where this effect is most pronounced. The percentage of Tc in outer belts was highest in cities such as Genoa, Trieste, and Trento where SUHI intensity was around and above 4 °C. Even in the suburban and rural areas, Tc percentage was higher in cities with more pronounced SUHI intensity.

Previous studies have established that increased vegetation (mainly Tc) in rural areas significantly contributes to increased daytime SUHI intensity (Yao et al., 2019). This correlation suggests that reducing greening, such as Tc, in rural areas or outer belts could mitigate SUHI by reducing its intensity between rural/outer belts and urban/central belts. However, this approach would not lower urban ST but would instead warm rural areas, equalizing temperatures across the municipality without cooling urban areas.

Moreover, urban reforestation interventions in central belts are challenging due to urban planning constraints, including space limitations and morphological factors, which generally make such interventions nearly impossible. This is particularly true for Italian cities, where historical and cultural preservation further limits such changes.

Conversely, increasing greening (such as Tc) in outer belts or rural areas is more feasible. Increased Tc in these areas can reduce ST and bring positive impacts in mitigating SUHI. Rural land cover surrounding a city can act as a natural absorber of urban heat, providing significant potential for mitigating the UHI effect on a citywide scale (Yang et al., 2024). Other factors, such as city structure, municipal area morphology, city center dimensions, and building heights, also influence UHI and heat distribution across the city.

In the dynamic heat exchange process between urban and rural environments, rural land cover, such as Tc, offers a unique opportunity to address UHI by utilizing neighboring rural areas to help reduce urban temperatures (Yang et al., 2024). Moreover, another study (Zou et al., 2021) found that UHI intensity increased during heat waves in highly urbanized areas, while less urbanized areas experienced improved cooling effects. These cooling effects are attributed to increased latent heat consumption by vegetation, such as Tc, during heat waves (Zou et al., 2021).

5. Conclusion

This study conducted a comprehensive analysis of summer SUHI phenomenon across Italian regional capitals using remote sensing data. The two methodologies adopted revealed the presence of SUHI in the Italian regional capitals, showing different intensities. Notably, the urbanization level approach exhibited higher SUHI intensity values. Moreover, the percentage of Tc in outer areas or belts proved useful in assessing a positive correlation between Tc and SUHI intensity, particularly in plain cities, according to the OMI approach.

This research is part of the MIRIFICUS project, which aims to enhance the understanding of the SUHI phenomenon across Italy through remote sensing data and to provide and share such information for public utility.

The results of this study will be used to assist Public Administrations that have expressed interest in the MIRIFICUS Project (including the National Association of Italian Municipalities, the Municipality of Rome Capital, and Florence) in urban planning and reforestation strategies.

Further investigations could expand the study period to include seasonal variations and nighttime assessments, as well as analyzing surface thermal anomalies in regional capitals where the SUHI phenomenon is most intense. Expanding the scope in this manner would contribute to a more comprehensive understanding of the SUHI phenomenon in Italy.

CRediT authorship contribution statement

Gennaro Albini: Writing – original draft, Validation, Methodology, Investigation, Formal analysis, Data curation, Conceptualization. **Giulia Guerri:** Writing – review & editing, Software, Methodology, Formal analysis, Conceptualization. **Michele Munafò:** Writing – review & editing, Visualization, Supervision, Conceptualization. **Marco Morabito:** Writing – review & editing, Visualization, Supervision, Resources, Methodology, Funding acquisition, Conceptualization.

Funding

This work was supported by the MIRIFICUS project (Monitoraggio degli Interventi di RIForestazione per l'Isola di Calore Urbana tramite i Satelliti), funded by the Italian Space Agency (ASI), Call for Ideas "Effects of climate change and extreme events"- "I4DP_PA (INNOVATION FOR DOWNSTREAM PREPARATION FOR PUBLIC ADMINISTRATIONS)", Agreement No. 2023-34-HH.0 of June 30, 2023.

Declaration of competing interest

The authors declare that they have no known competing financial interests or personal relationships that could have appeared to influence the work reported in this paper.

Acknowledgements

This research is part of the MIRIFICUS project, funded and supported by the Italian Space Agency (ASI). The authors wish to express their gratitude to the MIRIFICUS working group (listed at https://mirificus.isprambiente.it/home/Le_persone.html) for their valuable collaboration throughout the project. The authors acknowledge the European Space Agency and the USGS–NASA for providing Sentinel-1 and -2 and Landsat-8 and -9 data and products related to the summer period from 2013 to 2023. Special thanks to the Italian National Institute for Environmental Protection and Research (ISPRA) for providing the high-resolution tree-cover, grassland, and impervious-surface layers used in this study. The authors also thank the National Revenue Agency of Italy for providing data on Italian regional capital municipalities.

Appendix A. Supplementary data

Supplementary data to this article can be found online at https://doi.org/10.1016/j.rsase.2025.101567.

Data availability

Data will be made available on request.

References

Adeyeri, O.E., Akinsanola, A.A., Ishola, K.A., 2017. Investigating surface urban heat island characteristics over Abuja, Nigeria: relationship between land surface temperature and multiple vegetation indices. Remote Sens. Appl.: Soc. Environ. 7, 57–68. https://doi.org/10.1016/j.rsase.2017.06.005. ISSN 2352-9385.

Akbari, H., Kolokotsa, D., 2016. Three decades of urban heat islands and mitigation technologies research. Energy Build. 133, 834–842. https://doi.org/10.1016/j.enbuild.2016.09.067.

Barbieri, T., Despini, F., Teggi, S., 2018. A multi-temporal analyses of land surface temperature using landsat-8 data and open source software: the case study of modena, Italy. Sustainability 10, 1678. https://doi.org/10.3390/su10051678.

Battaglia, J.M.A., Douglas, S., Hennigan, C.J., 2017. Effect of the urban heat island on aerosol pH. Environ. Sci. Technol. 51, 13095–13103. https://doi.org/10.1021/acs.est.7b02786.

Bonafoni, S., Anniballe, R., Pichierri, M., 2015. Comparison between surface and canopy layer urban heat island using MODIS data. Joint Urban Remote Sens. Event (JURSE) 1–4. https://doi.org/10.1109/JURSE.2015.7120457. Lausanne, Switzerland.

De Fioravante, P., et al., 2021. Multispectral sentinel-2 and SAR sentinel-1 integration for automatic land cover classification. Land 10, 611. https://doi.org/10.3390/land10060611.

De Fioravante, P., et al., 2022. High resolution land cover integrating Copernicus products: a 2012–2020 map of Italy. Land 11, 35. https://doi.org/10.3390/land11010035.

Dewan, A., et al., 2021. Surface urban heat island intensity in five major cities of Bangladesh: patterns, drivers and trends. Sustain. Cities Soc. 71, 102926. https://doi.org/10.1016/j.scs.2021.102926.

De Razza, S., et al., 2024. Mapping urban heatwaves and islands: the reverse effect of Salento's "white cities". Front. Earth Sci. 12, 1375827. https://doi.org/10.3389/feart.2024.1375827.

Esposito, A., et al., 2024. Urban morphology and surface urban heat island relationship during heat waves: a study of milan and lecce (Italy). Remote Sens. 16, 4496. https://doi.org/10.3390/rs16234496.

Festa, M., et al., 2017. Manuale della Banca dati Quotazioni Dell'osservatorio del Mercato Immobiliare. Istruzioni Tecniche per la Formazione della Banca Dati Quotazioni OMI. Agenzia delle Entrate, Rome, Italy. Available online: https://www.agenziaentrate.gov.it/wps/content/nsilib/nsi/schede/fabbricatiterreni/omi/manuali+e+guide. (Accessed 10 December 2024).

Fioravanti, G., et al., 2022a. I normali climatici 1991-2020 di temperatura e precipitazione in Italia, Rapporto ISPRA/Stato dell'Ambiente 99/2022.

Fioravanti, G., et al., 2022b. Gli indicatori del Clima in Italia 2021 Anno XVII, ISPRA, Stato dell'Ambiente 98/2022b. ISBN 978-88-448-1119-8.

Firozjaei, M.K., et al., 2023. Seasonal and daily effects of the sea on the surface urban heat island intensity: a case study of cities in the Caspian Sea Plain. Urban Clim. 51, 101603. https://doi.org/10.1016/j.uclim.2023.101603. ISSN 2212-0955.

Fratianni, S., Acquaotta, F., 2017. The climate of Italy. In: Soldati, M., Marchetti, M. (Eds.), Landscapes and Landforms of Italy. *World Geomorphological Landscapes*. Springer, Cham, pp. 29–38. https://doi.org/10.1007/978-3-319-26194-2_4.

Giorgi, F., Lionello, P., 2008. Climate change projections for the Mediterranean region. Global Planet. Change 63 (Issues 2–3), 90–104. https://doi.org/10.1016/j.gloplacha.2007.09.005. ISSN 0921-8181.

Grigoras, G., Uritescu, B., 2018. Spatial hotspot analysis of bucharest's Urban Heat Island (UHI) using modis data, annals of Valahia University of Targoviste. Geogr Ser. 18, 14–22. https://doi.org/10.2478/avutgs-2018-0002.

Guerri, G., et al., 2021. Thermal summer diurnal hot-spot analysis: the role of local urban features layers. Remote Sens. 13, 538. https://doi.org/10.3390/rs13030538.

Guha, S., et al., 2018. Analytical study of land surface temperature with NDVI and NDBI using Landsat 8 OLI and TIRS data in florence and Naples city, Italy. Euro. J. Remote Sen. 51, 667–678. https://doi.org/10.1080/22797254.2018.1474494.

Guo, F., et al., 2023. Effects of urban form on sea cooling capacity under the heatwave. Sustain. Cities Soc. 88, 104271. https://doi.org/10.1016/j.scs.2022.104271. ISSN 2210-6707.

Hidalgo-García, D., Arco-Díaz, J., 2022. Modeling the Surface Urban Heat Island (SUHI) to study of its relationship with variations in the thermal field and with the indices of land use in the metropolitan area of Granada (Spain). Sustain. Cities Soc. 87, 104166. https://doi.org/10.1016/j.scs.2022.104166. ISSN 2210-6707.

Hjort, J., et al., 2022. Impacts of permafrost degradation on infrastructure. Nat. Rev. Earth Environ. 3, 24–38. https://doi.org/10.1038/s43017-021-00247-8.

IPCC, 2022. Climate change 2022: impacts, adaptation, and vulnerability. Contrib. Work. Group II Sixth Assess. Rep. Intergov. Panel Clim. Change 3056. https://doi.org/10.1017/9781009325844. Cambridge University Press, Cambridge, UK and New York, NY, USA.

ISTAT - Italian National Institute of Statistics, 2024. Principali statistiche geografiche sui comuni. https://www.istat.it/classificazione/principali-statistiche-geografiche-sui-comuni/.

Marando, F., et al., 2022. Urban heat island mitigation by green infrastructure in European Functional Urban Areas. Sustain. Cities Soc. 77, 103564. https://doi.org/10.1016/j.scs.2021.103564. ISSN 2210-6707.

Mentaschi, L., et al., 2022. Global long-term mapping of surface temperature shows intensified intra-city urban heat island extremes. Glob. Environ. Change 72, 102441. https://doi.org/10.1016/j.gloenvcha.2021.102441. ISSN 0959-3780.

Mirzaei, M., et al., 2020. Urban heat island monitoring and impacts on citizen's general health status in isfahan metropolis: a remote sensing and field survey approach. Remote Sens. 12, 1350. https://doi.org/10.3390/rs12081350.

Morabito, M., et al., 2018. Urban imperviousness effects on summer surface temperatures nearby residential buildings in different urban zones of parma. Remote Sens. 10, 26. https://doi.org/10.3390/rs10010026.

Morabito, M., et al., 2021. Surface urban heat islands in Italian metropolitan cities: tree cover and impervious surface influences. Sci. Total Environ. 751, 142334. https://doi.org/10.1016/j.scitotenv.2020.142334.

Munafò, M., 2023. Consumo di suolo, dinamiche territoriali e servizi ecosistemici. Edizione 2023. Report SNPA 37/23.

Nicholls, R.J., Hoozemans, F.M.J., 1996. The Mediterranean: vulnerability to coastal implications of climate change. Ocean Coast Manag. 31 (Issues 2–3), 105–132. https://doi.org/10.1016/S0964-5691(96)00037-3. ISSN 0964-5691.

Oke, T.R., 1987. Boundary Layer Climates, second ed. Methuen Co., London, New York, p. 435.

Phan, K.D., et al., 2024. Remote sensing for urban heat island research: progress, current issues, and perspectives. Remote Sens. Appl.: Soc. Environ. 33, 101081. https://doi.org/10.1016/j.rsase.2023.101081. ISSN 2352-9385.

Pisano, A., et al., 2020. New evidence of mediterranean climate change and variability from sea surface temperature observations. Remote Sens. 12, 132. https://doi.org/10.3390/rs12010132.

QGIS Development Team, 2023. QGIS Geographic Information System. Open source geospatial foundation project. Available online: http://qgis.osgeo.org. (Accessed 10 December 2024).

Ribeiro, A.P., et al., 2023. The role of tree landscape to reduce effects of urban heat islands: a study in two Brazilian cities. Trees (Berl.) 37, 17–30. https://doi.org/10.1007/s00468-021-02230-8.

Roberts, D.A., et al., 2012. Synergies between VSWIR and TIR data for the urban environment: an evaluation of the potentialfor the hyperspectral infrared imager (HyspIRI) decadal survey mission. Rem. Sens. Environ. 117, 83–101. https://doi.org/10.1016/j.rse.2011.07.021.

Rubel, F., Kottek, M., 2010. Observed and projected climate shifts 1901-2100 depicted by world maps of the Köppen-Geiger climate classification. Meteorol. Z. 19, 135–141. https://doi.org/10.1127/0941?2948/2010/0430.

RStudio Team, 2020. RStudio. Integrated Development for R. RStudio, PBC, Boston, MA. http://www.rstudio.com. (Accessed 10 December 2024).

Saha, S., et al., 2021. Analyzing spatial relationship between land use/land cover (LULC) and land surface temperature (LST) of three urban agglomerations (UAs) of Eastern India. Remote Sens. Appl.: Soc. Environ. 22, 100507. https://doi.org/10.1016/j.rsase.2021.100507. ISSN 2352-9385.

Seneviratne, S.I., et al., 2021. Weather and climate extreme events in a changing climate. In: Masson-Delmotte, V., et al. (Eds.), Climate Change 2021: the Physical Science Basis. Contribution of Working Group I to the Sixth Assessment Report of the Intergovernmental Panel on Climate Change. Cambridge University Press, pp. 1513–1766. https://doi.org/10.1017/9781009157896.013.

Siswanto, S., et al., 2023. Spatio-temporal characteristics of urban heat Island of Jakarta metropolitan. Remote Sens. Appl.: Soc. Environ. 32, 101062. https://doi.org/10.1016/j.rsase.2023.101062. ISSN 2352-9385.

Stewart, I.D., et al., 2021. Time evolution of the surface urban heat island. Earths Future 9 (10), e2021EF002178. https://doi.org/10.1029/2021EF002178.

Stolte, T.R., et al., 2024. VulneraCity–drivers and dynamics of urban vulnerability based on a global systematic literature review. Int. J. Disaster Risk Reduct. 108 (2024), 104535. https://doi.org/10.1016/j.ijdrr.2024.104535. ISSN 2212-4209.

Tan, Z., Ka-Lun Lau, K., Ng, E., 2016. Urban tree design approaches for mitigating daytime urban heat island effects in a high-density urban environment. Energy Build. 114, 265–274. https://doi.org/10.1016/j.enbuild.2015.06.031. ISSN 0378-7788.

The World Bank, 2024. Open Data Indicators. https://data.worldbank.org/. (Accessed 10 December 2024).

World Health Organization, Regional Office for Europe, 2021. Heat and health in the WHO European Region: updated evidence for effective prevention. World Health Organization. Regional Office for Europe. https://iris.who.int/handle/10665/339462. License: CC BY-NC-SA 3.0 IGO.

Yao, R., et al., 2019. Greening in rural areas increases the surface urban heat island intensity. Geophys. Res. Lett. 46 (4), 2204–2212. https://doi.org/10.1029/2018GL081816.

Yang, J., et al., 2020. Investigating the diversity of land surface temperature characteristics in different scale cities based on local climate zones. Urban Clim. 34, 100700. https://doi.org/10.1016/j.uclim.2020.100700.

Yang, M., et al., 2024. Mitigating urban heat island through neighboring rural land cover. Nat. Cities 1, 522–532. https://doi.org/10.1038/s44284-024-00091-z.

Zhao, Z.Q., et al., 2017. Profile and concentric zonal analysis of relationships between land use/land cover and land surface temperature: case study of Shenyang, China. Energy Build. 155, 282–295. https://doi.org/10.1016/j.enbuild.2017.09.046.

Zargari, M., et al., 2024. Climatic comparison of surface urban heat island using satellite remote sensing in Tehran and suburbs. Sci. Rep. 14, 643. https://doi.org/10.1038/s41598-023-50757-2.

Zhou, D., et al., 2014. Surface urban heat island in China's 32 major cities: spatial patterns and drivers. Rem. Sens. Environ. 152, 51–61. https://doi.org/10.1016/j.rse.2014.05.017. ISSN 0034-4257.

Zou, Z., et al., 2021. Impacts of land use/land cover types on interactions between urban heat island effects and heat waves. Build. Environ. 204, 108138. https://doi.org/10.1016/j.buildenv.2021.108138. ISSN 0360-1323.